

# On the Wong cross section and fusion oscillations

N. Rowley<sup>1</sup> and K. Hagino<sup>2,3</sup>

<sup>1</sup>UMR 8608, Institut de Physique Nucléaire, 91406 Orsay Cedex, France

<sup>2</sup>Department of Physics, Tohoku University, Sendai 980-8578, Japan

<sup>3</sup>Research Center for Electron Photon Science, Tohoku University, 1-2-1 Mikamine, Sendai 982-0826, Japan

We re-examine the well-known Wong formula for heavy-ion fusion cross sections. Although this celebrated formula yields almost exact results for single-channel calculations for relatively heavy systems such as  $^{16}\text{O}+^{144}\text{Sm}$ , it tends to overestimate the cross section for light systems such as  $^{12}\text{C}+^{12}\text{C}$ . We generalise the formula to take account of the energy dependence of the barrier parameters and show that the energy-dependent version gives results practically indistinguishable from a full quantal calculation. We then examine the deviations arising from the discrete nature of the intervening angular momenta, whose effect can lead to an oscillatory contribution to the excitation function. We recall some compact, analytic expressions for these oscillations, and highlight the important physical parameters that give rise to them. Oscillations in symmetric systems are discussed, as are systems where the target and projectile identities can be exchanged via a strong transfer channel.

PACS numbers: 25.70.Jj,25.70.Bc,25.70.Hi,24.10.-i

## I. INTRODUCTION

It has been known for many years that fusion cross sections for several light heavy-ion systems, such as  $^{12}\text{C}+^{12}\text{C}$  (Ref. [1]),  $^{12}\text{C}+^{16}\text{O}$  (Ref. [2]) and  $^{16}\text{O}+^{16}\text{O}$  (Ref. [3]), exhibit an oscillatory structure as a function of the incident energy. Two recent papers by Esbensen [4] and Wong [5] interpret the oscillations as due to the addition of successive individual partial waves as the energy increases. The effect is of course most important for identical spin-zero nuclei, because in that case the odd partial waves are totally absent and the relevant energy spacing between successive contributing angular momenta is consequently much larger. Both of these authors discuss this phenomenon in the context of the well-known Wong fusion cross section [6] derived from the Hill-Wheeler expression [7] for the penetration of a parabolic potential barrier. See also Ref. [8] for a recent publication in a similar context.

In fact the above interpretation was first proposed some 30 years ago by Poffé, Rowley and Lindsay [9] who, furthermore, gave a compact and accurate analytic expression for the oscillations that displays succinctly the dependence on the relevant physical parameters of the system. Our purpose in this paper is to discuss the derivation of the Wong cross section – both its smooth and oscillatory terms – and to present some inadequacies of the standard fusion formula that treats the barrier height, position and curvature  $[B, R_B, \hbar\omega]$  as independent of the incident energy  $E$  and thus, implicitly, independent of the angular momentum  $l$ .

This re-analysis of the qualities and weaknesses of the Wong formula is important in order to be able to distinguish between discrepancies arising from the approximations used in its derivation and those arising from additional physical effects such as entrance-channel couplings or limitations on compound-nucleus formation.

The paper is organized as follows. In Sec. II, we derive

the Wong cross section and propose an extended formula which takes into account the energy dependence of the barrier parameters. We show that the effect of the energy dependence is significant, particularly for light heavy-ion systems, and that the generalised formula reproduces well a full quantal calculation. In Sec. III, we discuss the oscillatory part of fusion cross sections. We re-analyze the compact formula for these oscillation using the energy-dependent version of the Wong formula. We discuss the fusion of two identical nuclei as well as fusion between similar nuclei. Fusion oscillations in heavier systems are also discussed. In Sec. IV, we present our analyses of the experimental data for the  $^{12}\text{C}+^{12}\text{C}$  and  $^{12}\text{C}+^{13}\text{C}$  systems. We summarize the paper in Sec. V.

## II. WONG FORMULA FOR FUSION CROSS SECTIONS AND ITS IMPROVEMENT

In this section, we compare the results of the Wong expression for the fusion cross section that contains the three parameters  $[B, R_B, \hbar\omega]$  (see below) and the fusion cross section coming from a quantal calculation with a specified real potential and an absorption that is essentially *black box*. This can be achieved either with an ingoing-wave boundary condition or with an appropriately chosen imaginary potential. Here we choose the latter method, checking carefully that our results are insensitive to changes in the imaginary potential used. With a potential model, the barrier position  $R_B$ , its height  $B$  and its curvature  $\hbar\omega$  are all fixed by the potential parameters. Indeed it is a very general result that the nuclear potential is essentially exponential in the tail, the region in which the Coulomb barrier occurs, at least for relatively light systems with low  $Z_1 Z_2$ . In that case, all three of the above parameters are determined by two potential parameters, the depth  $V_0$  and the surface diffuseness  $a$ .

We choose to fix these parameters in the following,

much more transparent way: for the  $l = 0$  barrier we have

$$\frac{dV}{dr} \Big|_{r=R_B} = \frac{dV_N}{dr} \Big|_{r=R_B} + \frac{dV_C}{dr} \Big|_{r=R_B} = 0, \quad (1)$$

where  $R_B$  is the position of the barrier. Writing  $V_N(r) = V_0 \exp[-(r - R_B)/a]$ , we then find

$$\frac{Z_1 Z_2 e^2}{R_B^2} - \frac{1}{a} V_0 = 0, \quad (2)$$

thus obtaining

$$V_N(r) = -\frac{a Z_1 Z_2 e^2}{R_B^2} \exp\left(-\frac{r - R_B}{a}\right). \quad (3)$$

Furthermore, we then have a Coulomb plus nuclear barrier

$$B = V(R_B) = \frac{Z_1 Z_2 e^2}{R_B} \left(1 - \frac{a}{R_B}\right), \quad (4)$$

and this quadratic equation for  $R_B$  gives the barrier position as

$$R_B = \frac{1}{2} R_C \left(1 + \sqrt{1 - 4 \frac{a}{R_C}}\right), \quad (5)$$

where  $R_C$  is just  $Z_1 Z_2 e^2 / B$  [45]. We see that once the barrier height  $B$  is given, the position depends only on the surface diffuseness of the potential, and this also fixes the strength of the nuclear potential. This is the reason that it is generally sufficient to quote the parameters  $[B, a]$  in our coupled-channels (CCFULL [10]) calculations. It is of course also sufficient for simpler optical-model/classical calculations of the fusion cross section. This procedure is useful because the parameter best determined by the fusion data is  $B$ , and furthermore there are various prescriptions for obtaining a good theoretical value for this quantity; for example the Bass [11] and the Akyüz-Winther [12] potentials that give very similar  $B$  values over a wide range of heavy-ion systems, both yielding  $B = 6.1$  MeV for the  $^{12}\text{C}+^{12}\text{C}$  system mainly discussed in this paper.

As noted above, this reduces the three independent parameters of the Wong expression to two, thereby providing a much more rigorous constraint on the physics of the problem, as we shall see below. Notice that the exponential potential tends to be deep, and such deep potentials have been advocated in Refs. [13–15].

If all of the flux crossing the Coulomb barrier fuses, then the fusion cross section is given by

$$\sigma = \frac{\pi \hbar^2}{2mE} \sum_{l=0}^{\infty} (2l+1) T_l, \quad (6)$$

and using the Hill-Wheeler formula for the transmission  $T_l$  through a parabolic barrier, we have [6]

$$\sigma = \frac{\pi \hbar^2}{2mE} \sum_{l=0}^{\infty} \frac{2l+1}{1 + \exp\left[\frac{2\pi}{\hbar\omega} \left(B + \frac{l(l+1)\hbar^2}{2mR_B^2} - E\right)\right]}, \quad (7)$$

where in the barrier region, the potential is taken as  $V(r) = B + \frac{l(l+1)\hbar^2}{2mR_B^2} - \frac{1}{2}m\omega^2(r - R_B)^2$ . (The quantity  $\hbar\omega$  is the quantum of energy corresponding to the inverted barrier and is generally referred to as the ‘barrier curvature’ [see Eq. (13)].) Taking  $[B, R_B, \hbar\omega]$  as fixed, and replacing the summation by an integral, one obtains the very influential Wong formula for the fusion cross section for a single potential barrier

$$\sigma = \frac{\hbar\omega}{2E} R_B^2 \ln\left(1 + \exp\left[\frac{2\pi}{\hbar\omega}(E - B)\right]\right), \quad (8)$$

which yields, in the limit  $E - B \gg \hbar\omega/2\pi$ , the classical result

$$E\sigma = \pi R_B^2 (E - B). \quad (9)$$

The first and second derivatives of this classical equation and its quantal version yield

$$\frac{d(E\sigma)}{dE} = \pi R_B^2 \theta(E - B) \rightarrow \pi R_B^2 \frac{1}{1 + e^x} \quad (10)$$

and

$$\begin{aligned} \frac{d^2(E\sigma)}{dE^2} &= \pi R_B^2 \delta(E - B) \\ &\rightarrow \pi R_B^2 \left[ \frac{2\pi}{\hbar\omega} \frac{e^x}{(1 + e^x)^2} \right], \end{aligned} \quad (11)$$

where  $x = (2\pi/\hbar\omega)(B - E)$  and  $\theta$  is the Heaviside step function. These functions (especially the second) have been extremely important in the development of the notion of a fusion barrier distribution [16, 17], where the fact that  $d^2(E\sigma)/dE^2$  is strongly peaked near to the barrier is a crucial point.

It is important to notice that higher above the barrier, one must question the approximations that lead to Eq. (8). Figure 1 shows that for higher angular momenta the barrier in the full potential (Coulomb + nuclear + centrifugal) occurs at a separation  $R_E$  smaller than its  $l = 0$  value,  $R_B$ . Now the grazing angular momentum is given by

$$\frac{l_g(l_g+1)\hbar^2}{2mR_E^2} = E - V_E, \quad (12)$$

where  $V_E$  is the sum of the Coulomb and nuclear potentials at  $R_E$ . Of course the curvature changes too, not only because the position of the barrier has shifted, but also because there is now a centrifugal contribution:

$$\hbar\omega_E = \hbar \left(-\frac{V''}{m}\right)^{1/2} = \hbar \left(-\frac{V_C'' + V_N'' + V_l''}{m}\right)^{1/2}, \quad (13)$$

where the second derivatives are evaluated at  $r = R_E$ . A better approximation for the fusion cross section is now just

$$\sigma = \frac{\hbar\omega_E}{2E} R_E^2 \ln\left(1 + \exp\left[\frac{2\pi}{\hbar\omega_E}(E - V_E)\right]\right), \quad (14)$$

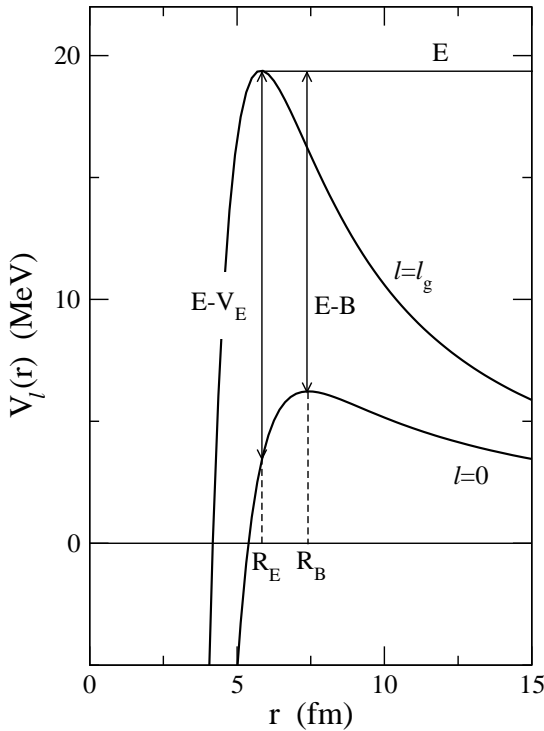


FIG. 1: For an incident energy  $E$  above the Coulomb barrier  $B$ , the radius for the barrier with grazing angular momentum  $l_g$  occurs at a separation  $R_E < R_B$ . The sum of the Coulomb and nuclear potentials at this point is  $V_E < B$ . Furthermore, the curvature  $\hbar\omega_E$  of the barrier in the total potential is larger than its value for  $l = 0$ . The curves are calculated for an exponential potential with  $a = 0.8$  fm and a depth that yields  $B = 6.22$  MeV for the  $^{12}\text{C} + ^{12}\text{C}$  system. For  $l = 0$  this potential has  $R_B = 7.44$  fm and  $\hbar\omega_E = 2.52$  MeV.

which is simply the standard Wong formula but with an energy-dependence  $[B, R_B, \omega] \rightarrow [V_E, R_E, \omega_E]$  derived for the grazing angular momentum  $l_g$  at the energy in question. See Ref. [18] for a similar extension to the classical formula, Eq. (9).

Of course we are still making an approximation here, because it is clear from Fig. 1 that the barrier height, position and curvature depend explicitly on  $l$ . Of course if one does not assume the same values of the parameters for all  $l$ , then the integral over  $l$  leading to Eq. (14) cannot be performed analytically. But there is nothing to prevent one choosing a different parameter set (for all  $l$ ) at each energy. Clearly the set of values for  $l_g$  is the best choice. One then still obtains the compact expression (14) though we should stress that one now needs to derive numerically the parameters  $[V_E, R_E, \omega_E]$  (see Appendix A).

We show in Fig. 2 some calculations for the system  $^{12}\text{C} + ^{12}\text{C}$  that we shall concentrate on in this paper. For the moment, they ignore the Bose symmetry of this identical spin-zero system and sum over all even *and* odd partial waves. The dashed line in Fig. 2 (a) shows the Wong cross section with  $[B, R_B, \omega]$  fixed at all en-

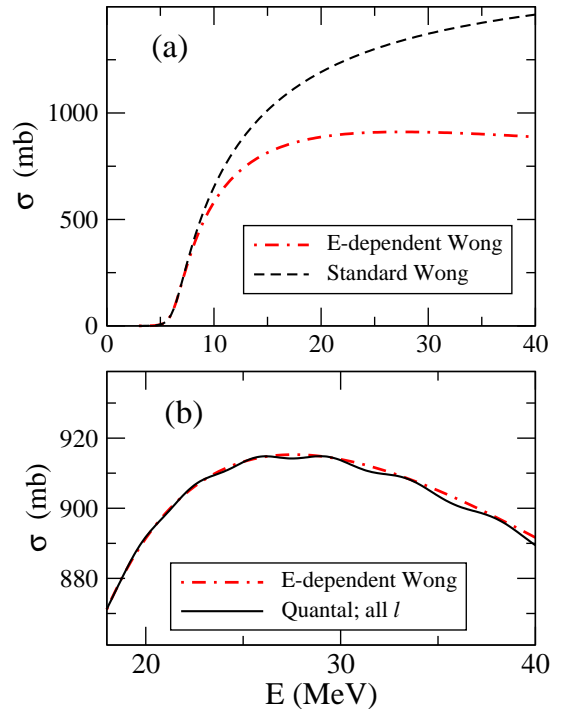


FIG. 2: (Color online) (a) Fusion cross sections for the  $^{12}\text{C} + ^{12}\text{C}$  system obtained with the Wong formula with  $l = 0$  values of  $[B, R_B, \hbar\omega]$  (dashed curve) and with their energy-dependent values (dot-dashed curve). The Bose symmetry of the identical spin-zero system is ignored, and both even and odd partial waves are summed up in the cross sections. (b) The energy-dependent Wong result agrees extremely well with a full quantal calculation shown by the solid line. However, the latter shows very weak oscillations ( $\approx 1$  mb) coming from the partial-wave sum (6) even though all  $l$  are summed.

ergies to their values for  $l = 0$ . That is  $[B, R_B, \omega] = [6.22 \text{ MeV}, 7.42 \text{ fm}, 2.52 \text{ MeV}]$ , generated by a potential with  $a = 0.8$  fm that gives this barrier height. The results are seen to be very different from the dot-dashed line that uses the energy-dependent values of these parameters. In Fig. 2 (b) we compare the latter results with a quantum mechanical calculation of the cross section. The scale of the vertical axis has been chosen to emphasise the high quality of the fit when the parameters are energy dependent. However, it also shows that even with all partial waves, there are small oscillations in the full quantal calculations. We shall derive an expression for these in the next section.

The following comments are appropriate at this point:

- The approximation with parameters fixed at their  $l = 0$  values is poor, especially for light systems. For these systems, the Coulomb interaction is relatively small and also the reduced mass  $m$  is small, therefore the centrifugal potential may play a more important role than the Coulomb potential. For heavier systems, on the other hand, the Coulomb potential is strong and thus the barrier is rigid

against a variation of angular momentum. In that situation, the conventional Wong formula is reasonable. Figure 3 shows the barrier position  $R_B$  and the barrier curvature  $\hbar\omega$  as a function of angular momentum  $l$  for two different systems,  $^{12}\text{C}+^{12}\text{C}$  and  $^{16}\text{O}+^{144}\text{Sm}$ . One can see that the variation is marginal for the heavier system,  $^{16}\text{O}+^{144}\text{Sm}$ , while both  $R_B$  and  $\hbar\omega$  change considerably as a function of  $l$  for the lighter system,  $^{12}\text{C}+^{12}\text{C}$ .

- However, note that experimental fusion cross sections (especially if they are not terribly precise) can frequently be fitted even for light heavy-ion systems with parameters that are simply chosen to do so, and do not necessarily bear much relation to the physical potential. For example, we shall see in Sec. III-D that the  $^{12}\text{C}+^{12}\text{C}$  experimental fusion cross section can be reasonably well fitted with  $[B, R_B, \hbar\omega] = [5.6, 6.3, 3.0]$  (see Fig. 8 below).
- The  $E$ -dependent Wong formula works well because the parabolic approximation is good, since the energy  $E$  coincides with the barrier height for  $l = l_g$ . Even though this approximation breaks down at energies below the barrier, only a small number of partial waves in the vicinity of  $l_g$  contribute. The cross section is relatively large above the barrier and the resulting discrepancies are small.
- At sub-barrier energies, there is no  $l_g$  as such, and the best one can do is to take the parameters for  $l=0$ , though one is already below the barrier for this value of  $l$ . For higher  $l$  values, the situation is worse, but taking an  $l$ -dependent value of the parameters does not improve matters, as the parabolic approximation is in any case intrinsically poor below the Coulomb barrier [19, 20]. Here the cross section is small, so the errors are relatively more important.

### III. FUSION OSCILLATIONS

#### A. Fusion of two identical nuclei

In most situations, the value of  $\hbar\omega$  is irrelevant at energies above the Coulomb barrier, simply determining the rate of fall-off for  $E < B$ . (Note that in that region the parabolic approximation itself will become inadequate at sufficiently low energies [19, 21].) However, (as first pointed out by Poffé *et al.* [9], and more recently in Refs. [4, 5]) there is a rather unique situation where  $\hbar\omega$  is important *above* the barrier, principally for light symmetric spin-zero systems (though see below for other examples). Here, only even values of the grazing angular momentum are allowed and their barriers may be sufficiently well separated in energy for their successive addition to the cross section to give rise to fusion oscillations.

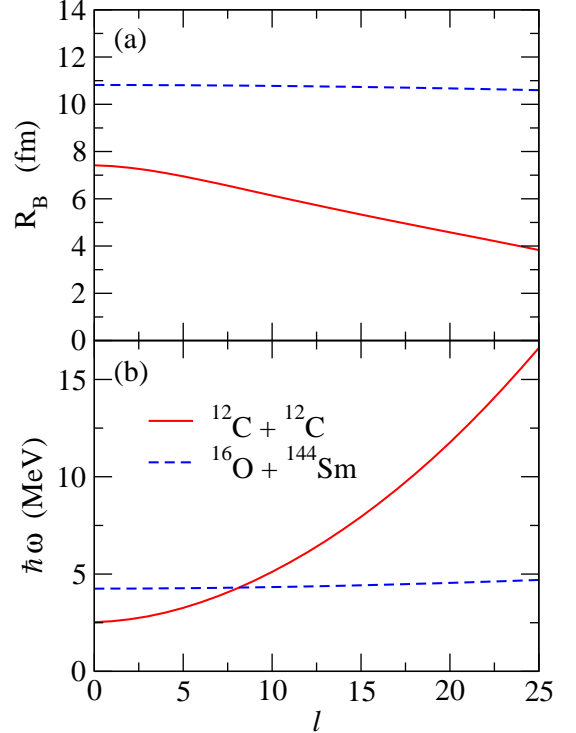


FIG. 3: (Color online) The barrier position,  $R_B$ , (upper panel) and the barrier curvature,  $\hbar\omega$ , (lower panel) as a function of angular momentum,  $l$ , for the  $^{12}\text{C}+^{12}\text{C}$  system (solid line) and the  $^{16}\text{O}+^{144}\text{Sm}$  system (dashed line).

Let us now derive the earlier expression of Poffé *et al.* [9] for these fusion oscillations. This is obtained by using the *exact* Poisson summation formula [22]

$$\sum_l f(l) = \sum_m (-1)^m \int_0^\infty f(\lambda) \exp(2\pi m i \lambda) d\lambda. \quad (15)$$

When applied to Eq. (7), the  $m = 0$  term gives the usual Wong result (14). The terms  $m = \pm 1$ , however, give rise to an oscillatory contribution from the poles of the transmission function above and below the real- $\lambda$  axis respectively. In the energy region  $E - B \gg \hbar\omega/2\pi$ , the nearest poles simply give (see Appendix B)

$$E\sigma_{\text{osc}} = 2\pi R_E^2 \hbar\omega_E \exp(-2\xi) \sin(2\pi l_g), \quad (16)$$

where  $l_g$  is the continuous, energy-dependent grazing angular momentum of Eq. (12), and the quantity  $\xi$  is given by

$$\xi = \frac{\hbar\omega_E}{2l_g + 1} \cdot \frac{\pi m R_E^2}{\hbar^2} \equiv \frac{\pi}{2} \frac{\hbar\omega_E}{\partial V_E / \partial l_g}. \quad (17)$$

The resultant oscillations are shown on top of the smooth part of the cross section in Fig. 2 (b). They are of the order of 1 mb, and it is unlikely that any reasonable experiment would be able to observe these. Terms from

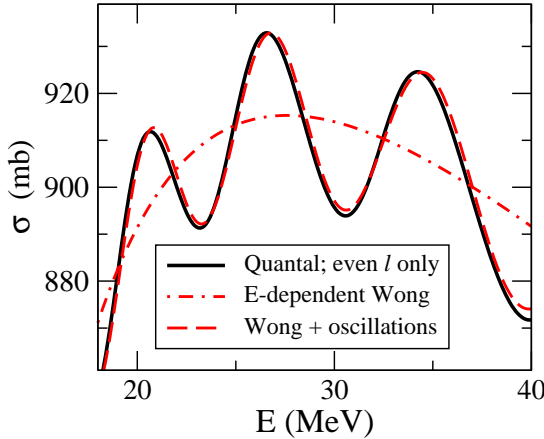


FIG. 4: (Color online) The symmetrised cross section (even  $l$  only) for  $^{12}\text{C} + ^{12}\text{C}$  is compared with the cross section for all  $l$ . One sees an order of magnitude difference in the oscillatory terms (see text). It is unlikely that the oscillations shown in Fig. 2 (b) ( $\approx 1 \text{ mb}$ ) could be observed in a system without some asymmetry between odd and even  $l$  values.

$|m| > 1$  and from more distant poles merely introduce higher multiples of the exponent in the above equation and are clearly completely negligible.

However, for a system of two identical spin-zero bosons (for example,  $^{12}\text{C} + ^{12}\text{C}$ ) the Bose symmetry forbids odd angular momenta, and the fusion cross section is given by twice the sum over the even partial waves. This can be achieved by including the factor

$$1 + [-1]^l \equiv 1 + \exp(\pi i l) \quad (18)$$

in Eq. (15). The 1 gives the usual non-symmetrised result but the extra term now gives an oscillatory contribution (from  $m = 0$  and  $m = -1$ ),

$$E\sigma_{\text{osc}} = 2\pi R_E^2 \hbar\omega_E \exp(-\xi) \sin(\pi l_g), \quad (19)$$

which is significantly larger than before, because the (negative) exponent has been reduced by a factor 2. This is demonstrated in Fig. 4, where the dashed curve represents the sum of the smooth, energy-dependent Wong cross section and the above expression for the oscillatory part. The solid curve is the full quantal calculation, and it can be seen that the above expressions give an excellent approximation to the exact result. The dot-dashed curve shows the smooth part of the Wong cross section. One sees an order-of-magnitude increase in the oscillations arising from symmetrisation.

The above result is easily generalised to two identical spin-1/2 fermions such as  $^{13}\text{C} + ^{13}\text{C}$ . Because the oscillatory cross section for odd partial waves is clearly just minus that for the even ones, the total  $\sigma_{\text{osc}}$  is simply given by the difference of the statistical weights for  $S = 0$  (which gives even  $l$  with weight 1/4) and for  $S = 1$  (giving odd  $l$  with weight 3/4). Thus we see that the oscillations will be reduced by a factor 2, and will have the opposite

phase from the symmetric system. Similarly, the oscillations for  $^{14}\text{N} + ^{14}\text{N}$  ( $1 \otimes 1$ ) will be reduced by a factor of 3 [9].

## B. Fusion between similar nuclei: the role of elastic transfer

The other interesting problem of this type is that of a system such as  $^{12}\text{C} + ^{16}\text{O}$ , which has also been discussed earlier by Kabir, Kermode and Rowley [23]. Here, one can again consider the oscillations from even  $l$  and odd  $l$  separately. Without any further effect, they will cancel out. However, the presence of the elastic  $\alpha$ -transfer channel will introduce a parity dependence into the problem. This is most easily seen by considering the total elastic scattering, where to the amplitude  $f_{\text{el}}(\theta)$  for direct elastic scattering of the  $^{12}\text{C}$ , we must add an exchange term  $f_{\text{trans}}(\pi - \theta)$ , the amplitude for elastic transfer at the angle and energy in question. This yields a total amplitude

$$f_{\text{total}}(\theta) \rightarrow f_{\text{el}}(\theta) + f_{\text{trans}}(\pi - \theta), \quad (20)$$

and using  $P_l(\cos(\pi - \theta)) = (-1)^l P_l(\cos \theta)$  we obtain

$$S_l^{\text{eff}} = S_l^{\text{el}} + (-1)^l S_l^{\text{trans}}, \quad (21)$$

that is, different effective  $S$ -matrix elements for the odd and even partial waves. This effect can be simulated (as in Refs. [23–28]) by introducing a parity-dependent optical potential. However, to obtain a simple orientation of the effect of transfer (and again an analytic expression for the oscillations) we note that the  $S$ -matrix for direct reactions is generally peaked around the grazing angular momentum and can be approximated by  $\alpha \partial S^{\text{el}} / \partial l$ . For relatively small  $\alpha$  (which is of course limited by unitarity), this gives an effective  $S$ -matrix

$$S^{\text{eff}}(l) = S^{\text{el}}(l + [-1]^l \alpha). \quad (22)$$

That is, the transfer dynamics results in a small shift of the original elastic  $S$ -matrix in *opposite directions* for odd and even  $l$  values. Clearly for a non-zero  $\alpha$  the poles giving rise to Eq. (19) come into play and indeed for  $\alpha=1/2$ , we obtain the same magnitude oscillations with a shift in phase. The general result is that the trigonometric function in Eq. (19) is replaced as follows

$$\begin{aligned} \sin(\pi l_g) &\rightarrow \frac{\sin(\pi[l_g + \alpha]) - \sin(\pi[l_g - \alpha])}{2} \\ &= \cos(\pi l_g) \sin(\pi \alpha). \end{aligned} \quad (23)$$

Of course in this expression  $\alpha$  may be energy dependent, and indeed if one uses a parity-dependent potential, this will naturally give rise to a shift that depends on the grazing  $l$  and thus on  $E$ . Ref. [23] demonstrated that it is possible to obtain a reasonable fit to both the large-angle elastic scattering and the fusion oscillations with the same parity-dependent potential.

### C. Heavier systems

The presence or absence of measurable fusion oscillations arising from the symmetrization for identical systems depends mainly on the quantity  $\xi$  in Eq. (17) because it appears in the exponent in Eq. (19). Using an exponential nuclear potential, Eq. (13) yields exactly

$$\hbar\omega_E = \hbar \left( \frac{2E - V_E - \frac{a}{R_E}\varepsilon}{a m R_E} \right)^{1/2}, \quad (24)$$

with  $\varepsilon \equiv 4(E - V_E) + V_{CE}$ , where  $V_{CE}$  is the Coulomb potential at  $R_E$ . Close to the s-wave barrier  $B$ , the nuclear potential is relatively small, and there  $\varepsilon \approx 4E - 3V_E$ . However, at higher energies and higher grazing  $l$  values, the barrier is pushed to lower radii and the nuclear potential gives the dominant contribution. Here  $V_{CE}$  can be neglected so that  $\varepsilon \approx 4(E - V_E)$  yielding

$$\xi \approx \frac{\pi}{2} \sqrt{\frac{R_E}{2a}} \left( \frac{2E - V_E}{E - V_E} - \frac{4a}{R_E} \right)^{1/2} \quad (25)$$

or in terms of  $B$

$$\xi \approx \frac{\pi}{2} \sqrt{\frac{R_E}{2a}} \left( 1 - \frac{4a}{R_E} + \left[ 1 - \frac{2a}{R_E} \right] \frac{E}{E - B} \right)^{1/2}. \quad (26)$$

Asymptotically ( $E \gg B$ ) this reduces to

$$\xi \approx \frac{\pi}{2} \sqrt{\frac{R_E}{a}} \left( 1 - \frac{3a}{R_E} \right)^{1/2}, \quad (27)$$

and this gives a good idea of the mass dependence of the magnitude of the resulting oscillations. For heavy systems,  $R_E$  is larger, and so is  $\xi$ . Thus the oscillations will become more difficult to observe experimentally in heavier systems.

The top panel of Fig. 5 compares the value of  $\xi$  for the  $^{12}\text{C}+^{12}\text{C}$  system (dot-dashed line) with that for  $^{28}\text{Si}+^{28}\text{Si}$  (solid line). For the former reaction, we have used the same potential as in Fig. 2, while we have used an exponential potential with  $[B, a] = [28.8 \text{ MeV}, 0.8 \text{ fm}]$  for the latter system. Even though the  $\xi$  parameter for  $^{28}\text{Si}+^{28}\text{Si}$  is larger than that for the  $^{12}\text{C}+^{12}\text{C}$  system by a factor of only about 2, its effect on the amplitude of the fusion oscillations is dramatic, as seen in the middle panel of Fig. 5. The oscillations shown here are obtained from Eq. (19) but they can also be simply obtained from the quantum mechanical sum over  $l$ : because the oscillations arising from symmetrization are exponentially larger than those with no symmetry, they are essentially given by the difference between these two cross sections. This reduces to

$$\sigma_{\text{osc}} = \frac{\pi\hbar^2}{2mE} \left( \sum_{l \text{ even}} (2l+1)T_l - \sum_{l \text{ odd}} (2l+1)T_l \right), \quad (28)$$

where we note that this result is true only if the sum over all partial waves is sufficiently smooth.

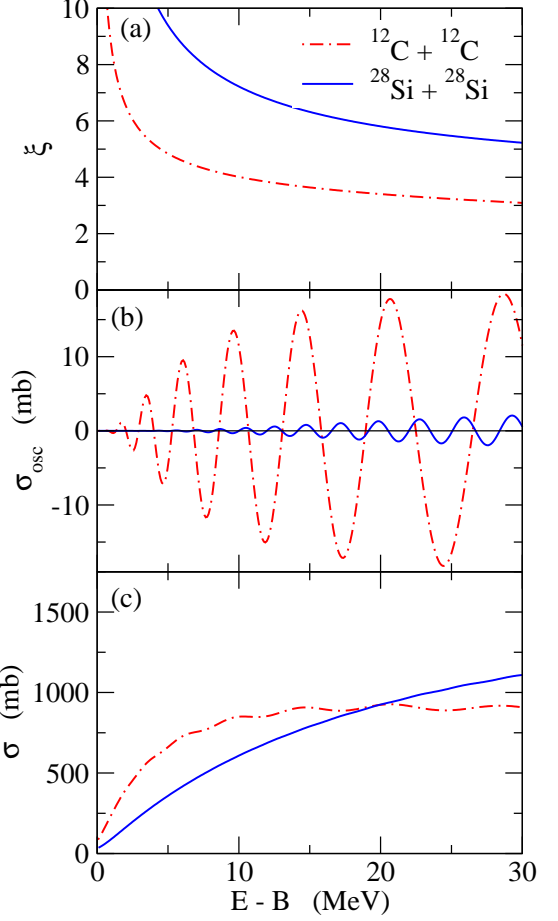


FIG. 5: (Color online) (a) The  $\xi$  parameter defined by Eq. (17) in the oscillatory part of fusion cross sections. The dot-dashed and the solid lines show the  $\xi$  parameters for the  $^{12}\text{C}+^{12}\text{C}$  system the  $^{28}\text{Si}+^{28}\text{Si}$  system, respectively, as a function of the energy measured from the barrier height  $B$  of each system. Both lines are obtained with an exponential potential with the diffuseness parameter of  $a=0.8 \text{ fm}$ . (b) The oscillatory contribution of fusion cross sections given by Eq. (19). (c) The total fusion cross sections for the two systems given as a sum of the smooth part and the oscillatory part.

Of course experimentally it is not possible to separate the oscillations out of the total cross section, and although they stand out in the  $^{12}\text{C}+^{12}\text{C}$  system (see bottom panel of Fig. 5), they are not apparent in the total cross section for  $^{28}\text{Si}+^{28}\text{Si}$ . For this reason the relevant experimental data are sometimes represented in the form of  $d(E\sigma)/dE$  [4]. This is a useful representation since the derivative of the smooth part of  $E\sigma$  is essentially constant. We shall look at this again below.

In the middle panel of Fig. 5, we have seen that the oscillations for the  $^{28}\text{Si}+^{28}\text{Si}$  system are largely damped out at energies less than around 10 MeV above the barrier, while they start much earlier, and are much stronger, for the  $^{12}\text{C}+^{12}\text{C}$  system. In order to understand this, Fig. 6 compares the derivative of the penetrability for

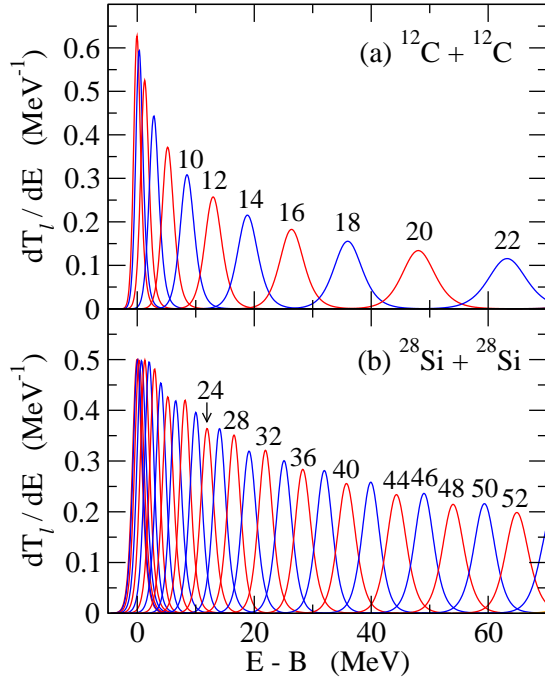


FIG. 6: (Color online) The first energy derivative of the penetrability for each angular momentum  $l$ ,  $dT_l/dE$ , for the  $^{12}\text{C}+^{12}\text{C}$  system (upper panel) and for the  $^{28}\text{Si}+^{28}\text{Si}$  system (lower panel). The numbers above the peaks are the corresponding values of  $l$ .

each angular momentum with respect to the energy, that is,  $dT_l/dE$ , for the  $^{12}\text{C}+^{12}\text{C}$  system (upper panel) with that for the  $^{28}\text{Si}+^{28}\text{Si}$  system (lower panel). For the latter system, the individual peaks are narrower (due to smaller values of  $\hbar\omega$ ), but they are pushed much closer together, making them less well resolved from the peaks for adjacent values of  $l$ . In order to obtain the same resolution that one has for  $l = 12$  in the  $^{12}\text{C}+^{12}\text{C}$  system (that is, the same degree of overlap between adjacent peaks), one has to go to an  $l$  value of around 36 or bigger in the  $^{28}\text{Si}+^{28}\text{Si}$  system. This corresponds to a much larger energy compared with the former system, and indeed the limiting angular momentum for fusion for  $^{28}\text{Si}+^{28}\text{Si}$  appears to be  $l_{\max} = 38$ , according to Vineyard *et al.* [29].

Several other data sets for the  $^{28}\text{Si}+^{28}\text{Si}$  system exist [30–32] and indeed one of the aims of Aguilera *et al.* [32] was to search for oscillations in this system. Unfortunately they were unable to conclude the existence of structures within the 3% statistical error in their experiment. Their data are represented in the form  $E\sigma$  in the upper panel of Fig. 7 (open circles), along with data from Ref. [30] (solid circles). It can be seen that the normalizations of the two data sets disagree somewhat, presumably simply due to systematic differences in the experiments. Also shown in the figure are two uncoupled optical-model calculations with  $a=0.6$  fm and 1.2 fm (both with  $B=28.7$  MeV). The slope of the former

fits that of the Aguilera data but the larger diffuseness is required to fit the slope of the data of Ref. [30]. In the lower panel of Fig. 7 the two data sets and calculations are again shown but in terms of  $d(E\sigma)/dE$ . Neither data set has the precision to prove the existence of oscillations, but it is interesting to note the significant difference in the magnitude of the oscillations produced by the different values of the potential diffuseness  $a$  (see Eq. (27)). Better data are clearly required to resolve this question, and to establish the existence or absence of any oscillations due to symmetrization.

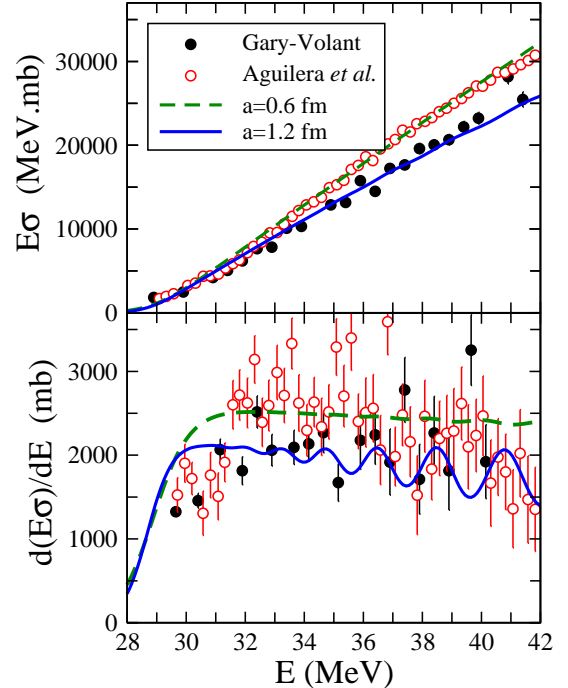


FIG. 7: (Color online) Two different sets of measurements [30, 32] for fusion in the  $^{28}\text{Si}+^{28}\text{Si}$  system are shown as  $E\sigma$  in the upper panel and as  $d(E\sigma)/dE$  in the lower one. The data are compared with uncoupled calculations with two different values of surface diffuseness in the nuclear potential. See text.

Very recently Stefanini *et al.* [33] have made more detailed measurements for this system with a very small energy step (around 0.25 MeV in the center-of-mass system) and with better statistics (better than 1%). Their experimental data, when displayed as  $d(E\sigma)/dE$ , indicate distinct structures at energies only around 5 MeV above the barrier. They are much more pronounced than those shown for the uncoupled calculation with  $a=1.2$  fm in Fig. 7. This observation is incompatible with the mechanism discussed here, and the oscillations in the new experimental data must have a different origin. Their presence appears to be related to strong couplings to the low-lying collective modes that exist in the  $^{28}\text{Si}$  nucleus, but also seems to depend on the nature of the absorptive potential used in the calculations [4, 33].

In order to look for the effects of channel cou-

plings, the ‘experimental barrier distribution’ [16, 17]  $D(E) = d^2(E\sigma)/dE^2$  is frequently used, and in the present context one should remember that the function  $d(E\sigma)/dE$  can also have structures close to the unperturbed Coulomb barrier due to couplings. The width of a typical barrier distribution is proportional to  $Z_1 Z_2$  and will lead to obvious structures in  $d(E\sigma)/dE$  for heavier systems with strong collective modes. However, for heavier systems, the ‘symmetrization’ oscillations will not be measurable. The system  $^{28}\text{Si}+^{28}\text{Si}$  may be a special intermediate system where both types of structure are present simultaneously.

#### IV. COMPARISON WITH EXPERIMENTAL DATA ON LIGHTER SYSTEMS

##### A. $^{12}\text{C}+^{12}\text{C}$ fusion reaction

Let us now analyze the actual experimental data for fusion of carbon isotopes and discuss the observed fusion oscillations. We first discuss the fusion of the  $^{12}\text{C}+^{12}\text{C}$  system using a single-channel optical model.

We have already shown in Fig. 3 the energy-dependence of the parameters  $R_E$  and  $\hbar\omega_E$  entering both the smooth part of the Wong cross section and its oscillatory term for the potential of Fig. 1 that gives a good fit to the experimental  $^{12}\text{C} + ^{12}\text{C}$  fusion cross section, including its oscillations. (Some of these energy variations have also been discussed in Ref. [18], where they are expressed in terms of universal functions.) The function  $dT_l/dE$  shown in the upper panel of Fig. 6 is for an optical-model calculation with the same potential and various  $l$  values. Its width is  $0.56 \hbar\omega_E$  [16], and this compares well with the values of  $\hbar\omega_E$  from Fig. 3, taken at the appropriate peak energies (where the  $l$  values in question are grazing). The variation of all of these Wong parameters is very significant over the energy range in question, and it is important to remember that their  $l = 0$  values do not even fit the average data when inserted into Eq. (14).

In Fig. 8, the data are reasonably well fitted [9, 20] (at least up to around 20 MeV) with an energy independent set of  $[B, R, \hbar\omega] = [5.6, 6.3, 3.0]$  but these parameters do not correspond to those coming from the potential-model fit shown in Fig. 9 (a). (Though the value of the oscillatory term is similar to the potential-model value in the region where the oscillations are important, because the expression (19) was used for it.) For instance, Eq. (4) indicates that this parameter set corresponds to an exponential potential with the diffuseness parameter of  $a = 2.0$  fm, that is unphysically large. The Wong cross section can, therefore, be considered only as providing a simple parametrisation of the fusion data, although as pointed out earlier this is extremely useful if one remains close to the barrier.

This point is well demonstrated by the failure to fit the cross section at energies above  $E \approx 25$  MeV, and

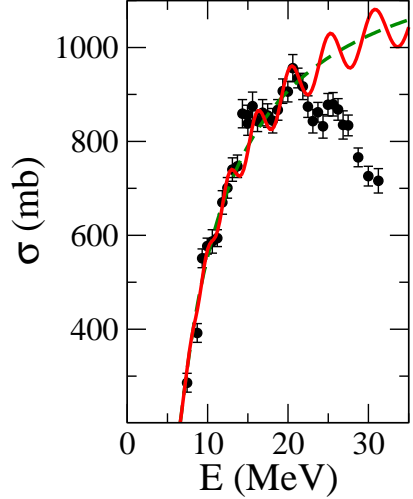


FIG. 8: (Color online) Parametrised  $^{12}\text{C}+^{12}\text{C}$  cross section [9, 20] with  $[B, R_B, \hbar\omega] = [5.6, 6.3, 3.0]$ . The smooth-only cross section is shown by the dashed curve. The experimental data are taken from Ref. [38].

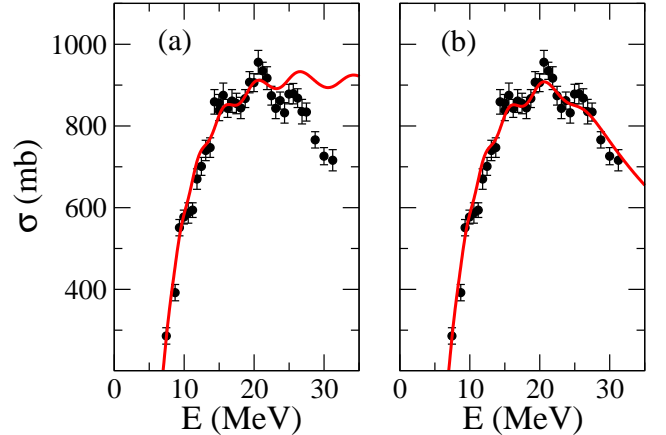


FIG. 9: (Color online) (a) Potential-model fit to the same data as in Fig. 8 with  $[B, a] = [6.22, 0.8]$  (even  $l$  only). (b) Same as (a) but with the transmission of  $l = 14$  reduced by a factor 2 and all higher waves absent.

Fig. 9 (b) shows that a likely explanation of this is the failure of higher partial waves to fuse. This fit is obtained with the transmission  $T_{l=14}$  reduced by a factor of 2, and all higher partial waves completely removed from the cross section.

Such an assumption is not unreasonable, because in this region of the compound nucleus spin  $I$ , the excitation energy of the  $^{24}\text{Mg}$  formed in the  $^{12}\text{C}+^{12}\text{C}$  reaction at the barrier height corresponding to an angular momentum  $l = I$ , is not sufficient for s-wave particle emission. That is,

$$Q + E_{\text{barrier}}(l) \equiv E_{\text{barrier}}^*(I = l) < E_{\text{yrast}}(I) + S_x, \quad (29)$$

where  $Q$  is the reaction  $Q$  value (13.93 MeV),  $E_{\text{yrast}}$  is the yrast energy of  $^{24}\text{Mg}$  [46], and  $S_x$  is the ap-

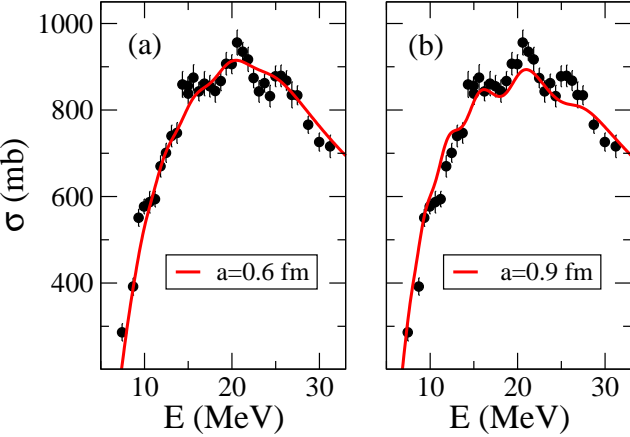


FIG. 10: (Color online) Fits to the  $^{12}\text{C}+^{12}\text{C}$  cross section with different potential parameters. The surface diffuseness  $a$  is constrained both by the magnitude of the smooth cross section and by the presence of oscillations. The left panel (a) shows results with  $a = 0.6$  fm and  $B = 6.54$  MeV, while the right panel (b) has  $a = 0.9$  fm and  $B = 6.06$  MeV. An intermediate value of  $a = 0.8$  fm appears best (see Fig. 9).

properite particle separation energy (where  $x \in$  neutron,  $S_n=16.53$  MeV; proton,  $S_p=11.69$  MeV; or alpha particle,  $S_\alpha=9.31$  MeV). But, for  $l \geq 12$  we find  $E_{\text{barrier}}^*(I=l) > E_{\text{yrast}}(I-1) + S_\alpha$ , permitting the emission of an  $L = 1$  alpha particle. Similarly for particle angular momentum  $L = 2$ , proton emission also becomes possible. However, such emissions are inhibited by the penetration of the corresponding centrifugal barriers as well as the relevant Coulomb barriers, and thus competition with fission will become important in the spin range above  $I=12$ .

In Fig. 10 we show potential model fits to the data with different values of the surface diffuseness  $a$ . While a good fit was obtained with  $a = 0.8$  fm as shown in Fig. 9 (b), Figs. 10 (a) and (b) show the best fits with slightly smaller and larger values  $a = 0.6$  fm and  $a = 0.9$  fm, respectively. In each case, the value of  $B$  is adjusted slightly to obtain the best fit and a clear pattern emerges. If one decreases  $a$  this increases  $R_B$  (Eq. (5)) which in turn increases the higher- $E$  cross section. This can be compensated by a slight increase in the barrier height which correspondingly decreases the radius again. Thus there is a little ‘play’ in the value of the potential parameters but one cannot stray too far from the ‘best’ values without destroying the fit either at higher or lower energies. Furthermore, the presence of the oscillations provides an additional strong constraint. For the smaller  $a$  value of 0.6 fm, the average cross section is fitted very well, but the magnitude of the oscillations is strongly damped. For the larger  $a$  value of 0.9 fm, the magnitude of the oscillations is increased (possibly improved) but the smooth part of the cross section starts to deviate. Thus we see that the data provide strong physical constraints on the physical properties of the nucleus-nucleus potential that

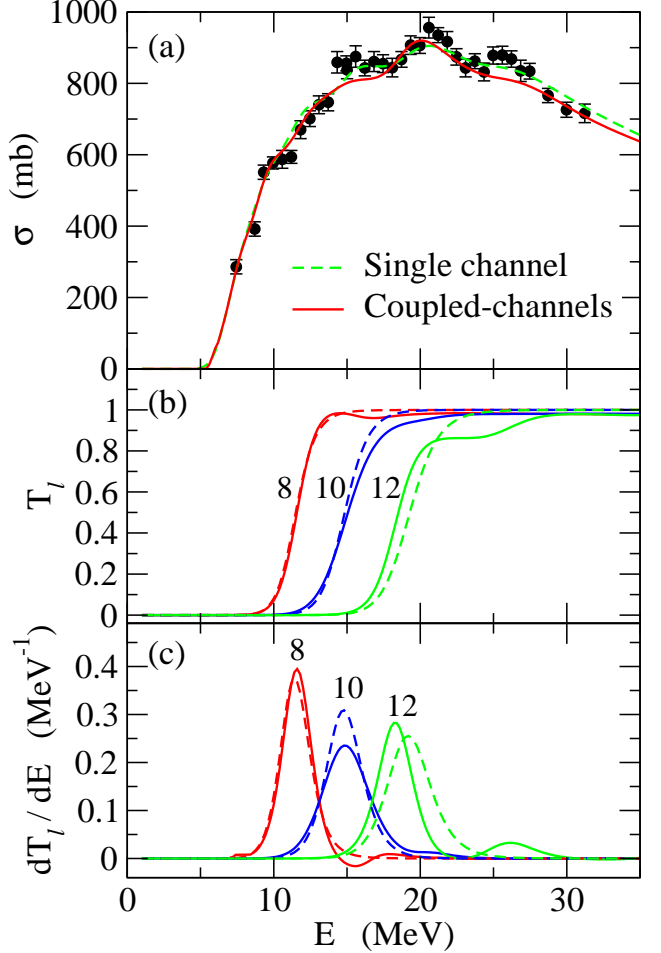


FIG. 11: (Color online) Effect of channel coupling on the fusion excitation function for the  $^{12}\text{C}+^{12}\text{C}$  system (top panel). The dashed line is the same as the solid line in Fig. 9 (b) obtained with the potential model. The solid line, on the other hand, is obtained by including the rotational coupling to the first  $2^+$  state both in the projectile and the target nuclei. The depth parameter of nuclear potential is slightly adjusted in order to remove the trivial barrier renormalization due to the couplings. The penetrability  $T_l$  and its first derivative  $dT_l/dE$  are shown in the middle and the bottom panels, respectively, for  $l = 8, 10$  and  $12$ .

are lost when the parameters  $[B, R_B, \hbar\omega]$  are regarded as independent variables. Thus while the elegance and simplicity of the Wong cross section should be recognised, so should its limitations.

So far we have discussed the fusion oscillations for the  $^{12}\text{C}+^{12}\text{C}$  system based on the single-channel potential-model calculations. In order to discuss the role of channel couplings, the top panel of Fig. 11 shows results of a coupled-channels calculation for the  $^{12}\text{C}+^{12}\text{C}$  system. To this end, we include the rotational coupling to the first  $2^+$  state both in the projectile and the target nuclei with the deformation parameter of  $\beta=-0.40$  [39] (with a radius parameter  $r_0=1.06$  fm). In order to remove the potential renormalization due to the coupling [20, 36, 37], we

slightly adjust the depth parameter of the nuclear potential. We use a modified version of CCFULL [10] to solve the coupled-channels equations. The solid and the dashed lines in Fig. 11 denote the results of the coupled-channels and the single-channel calculations, respectively. One can see that the main feature of the fusion oscillations, including the peak energies and the phase of the oscillations, are not affected much by the channel-coupling effects, and thus our discussions based on the simple potential model calculations remain valid.

This conclusion is due to the fact that the barrier distributions for non-zero  $l$  [4, 16, 20] still show almost a single-peaked structure, as shown in Figs. 11 (b) and (c). This originates from the following two reasons. Firstly the excitation energy of the  $2_1^+$  state in  $^{12}\text{C}$  is relatively large ( $E_2=4.44$  MeV) and thus the adiabatic approximation is good, leading to the adiabatic-barrier renormalization [20, 36, 37]. Secondly, with rotational coupling to an oblate nucleus, the lowest barrier, which is relevant to the adiabatic-barrier renormalization, carries most of the weight, as in the vibrational case. If  $^{12}\text{C}$  had a prolate deformation, the lowest barrier would have the smallest weight in the barrier distribution, and the fusion oscillations would be much more affected by the couplings. In that case, the oscillations are significantly damped, and thus the data essentially determine the sign of the deformation of  $^{12}\text{C}$ .

### B. $^{12}\text{C} + ^{13}\text{C}$ fusion reaction

Let us next discuss the  $^{12}\text{C} + ^{13}\text{C}$  systems, for which the effect of elastic neutron transfer is expected to play an important role. Based on the discussion in the previous subsection, we shall use the potential model for our discussions. Fig. 12 (a) shows the fusion cross section for this system and its fit with the Wong formula (dashed line). Although the oscillation is less prominent than for  $^{12}\text{C} + ^{12}\text{C}$ , the fusion cross section still shows significant oscillations and the Wong formula does not account well for them. The solid line in Fig. 12 (a) shows a fit with Eq. (19). Although the magnitude of the oscillatory structure is well reproduced, the oscillation is out of phase with the experimental data. Fig. 12 (b) shows a fit with Eq. (23) with  $\alpha=-0.5$ . It is apparent that this fit is better than the other two, and thus the experimental data appear to determine the relative phase of the transfer and elastic  $S$ -matrix elements.

Naturally, the sign of  $\alpha$  is related to the sign of a parity-dependent part of optical potential. In fact, if one introduces a parity-dependent barrier height,  $V_E \pm (-1)^l \Delta V$ , it is easy to show that the grazing angular momentum  $l_g$  is given to first order in  $\Delta V$  by

$$l_g = l_g^{(0)} \mp (-1)^l \frac{\Delta V_E}{2} \sqrt{\frac{2mR_E^2}{(E - V_E)\hbar^2}}, \quad (30)$$

where  $l_g^{(0)}$  is the grazing angular momentum for  $\Delta V=0$ .

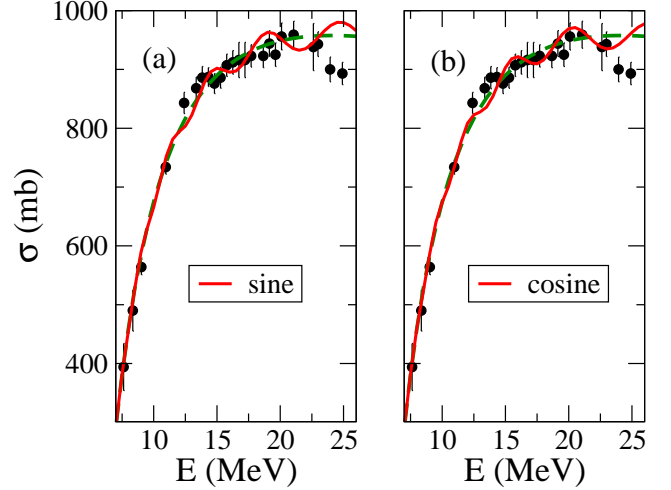


FIG. 12: (Color online) (a) Comparison between the experimental fusion excitation function and theoretical curves for the  $^{12}\text{C} + ^{13}\text{C}$  system. The dashed line is obtained with the Wong formula, while the solid line shows a fit to the data using Eq. (19). The experimental data are taken from Ref. [38]. (b) Same as (a) but with Eq. (23) and  $\alpha=-0.5$ .

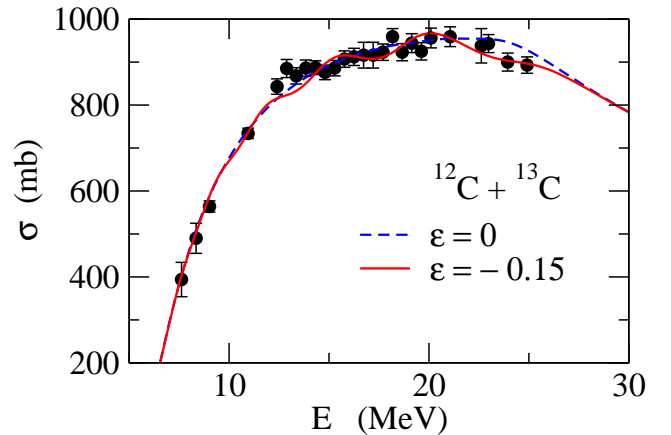


FIG. 13: (Color online) Fusion excitation function for  $^{12}\text{C} + ^{13}\text{C}$  obtained with a parity-dependent potential. The parity dependence is introduced by replacing  $V_0$  with  $V_0(1 + (-1)^l \epsilon)$  in the exponential potential  $V_N(r) = V_0 e^{-r/a}$ , where  $V_0$  takes a negative value. The solid and the dashed lines are obtained with  $\epsilon = -0.15$  and 0, respectively. The angular momentum sum is truncated at  $l = 14$  as in Fig. 9 (b).

This implies that  $\alpha$  is given by

$$\alpha = \mp(-1)^l \frac{\Delta V_E}{2} \sqrt{\frac{2mR_E^2}{(E - V_E)\hbar^2}}, \quad (31)$$

indicating that  $\alpha$  is positive (negative) if the barrier height for even-partial waves is lower (higher) than that for odd-partial waves. The negative sign of  $\alpha$  for the  $^{12}\text{C} + ^{13}\text{C}$  system suggests that the barrier for this system is lower for odd-partial waves. This is consistent

with earlier findings in Refs. [24, 27]. In Fig. 13, we show fusion cross sections obtained with a parity-dependent potential. The parity dependence is introduced by using an energy-dependent depth parameter,  $V_0(1 + (-1)^l \epsilon)$  in the exponential potential (here,  $V_0$  is defined as taking a negative value). The solid line in the figure indicates that the experimental data are well accounted for with  $\epsilon = -0.5$ , which indeed implies higher barriers for even partial waves.

In contrast to  $^{12}\text{C}+^{13}\text{C}$ , the quantity  $\alpha$  has been found to be positive for the  $^{12}\text{C}+^{16}\text{O}$  system [23], and we note that Baye [40] has proposed a simple rule for the sign of the parity-dependent potential in terms of the mass number  $A_{\text{core}}$  of the identical ‘cores’ of the colliding nuclei and the parities  $\pi_i$  of the valence orbitals of the transferred nucleons. His rule is based upon a microscopic resonating group method (RGM) within a two-center harmonic-oscillator shell model. Essentially the barrier for even partial waves is deemed to be higher (or lower) than that for odd partial waves if the quantity

$$-(-1)^{A_{\text{core}}} \prod_{i:\text{valence}} \pi_i \quad (32)$$

is positive (or negative). In both of our cases  $A_{\text{core}}$  is even. For  $^{12}\text{C}+^{16}\text{O}$  the number of valence particles is also even and this expression is negative. For the  $^{12}\text{C}+^{13}\text{C}$  reaction we have a single, odd-parity valence neutron ( $p_{1/2}$ ), and the expression is positive. The sign of  $\alpha$  determined from the fusion oscillations is consistent with these results for both of our systems.

Note that the sign of the parity-dependent term, obtained from a fit to the angular distribution of elastic scattering, shows some ambiguity for several systems [41]. Fusion oscillations may offer a direct and perhaps better way to determine the sign. We note, however, that even though the negative value of  $\alpha$  fits well the fusion oscillations and is consistent with the Baye’s rule, a positive value appears more consistent with the data for energies around 13 MeV (see Fig. 13). It would be interesting to re-measure fusion cross sections in this energy region with higher precision in order to confirm whether there exists a shift in phase of the oscillations as a function of energy.

## V. SUMMARY

The Wong formula has been widely used to estimate fusion cross sections for a given single-channel potential as well as to discuss the parameters which govern fusion. The formula is useful in discussing for example, the subbarrier enhancement of cross sections, providing reference cross sections in the absence of channel couplings. For relatively heavy systems, such as  $^{16}\text{O}+^{144}\text{Sm}$ , the formula indeed reproduces well the exact result except for the deep subbarrier region, where the parabolic approximation itself breaks down. On the other hand, for light systems, such as  $^{12}\text{C}+^{12}\text{C}$ , the Wong formula tends

to overestimate the cross section. In this paper, we have extended the Wong formula by including the energy dependence of the parameters entering the formula, that is, the barrier height, barrier position, and the barrier curvature. Evaluating these parameters at the grazing angular momentum for each energy, rather than at  $l = 0$ , we have shown that the energy-dependent version of Wong’s formula reproduces the exact result well, even for light systems.

The symmetrisation of the system leads to a Wong cross section possessing an oscillatory contribution, for which a compact formula can be derived based on the parabolic approximation. We have shown that the formula for the oscillatory contribution can also be extended to the energy-dependent version.

Fusion oscillations are most significant in light symmetric systems with spin-zero nuclei. We have analyzed the experimental data for the  $^{12}\text{C}+^{12}\text{C}$  system and have argued that the fusion oscillations provide a strong constraint on the nuclear potential employed in a calculation. We have also analysed the  $^{12}\text{C}+^{13}\text{C}$  system, in which elastic neutron transfer again gives rise to oscillations. We have shown that these oscillations are useful in determining the sign of the effective parity-dependent potential arising from elastic transfer.

We have argued that fusion oscillations provide an important tool for studying properties of the nuclear potential, strongly-coupled channels at high excitation energy, and fission. This is especially true for the  $^{12}\text{C}+^{12}\text{C}$  system, which plays an important role in several astrophysical phenomena and thus has been recognized as one of the key reactions [42–44] in that domain. Understanding both the smooth and oscillatory parts of the cross section above the barrier will almost certainly be necessary in understanding it in the important astrophysical region well below the barrier.

## Acknowledgments

This work was supported by JSPS KAKENHI Grant Number 25105503.

## Appendix A: Approximate formula for the energy-dependent barrier position

For the exponential potential of Eq. (3), the grazing angular momentum  $l_g$  is given by

$$E = -\frac{a Z_1 Z_2 e^2}{R_B^2} e^{\delta R/a} + \frac{Z_1 Z_2 e^2}{R_E} + \frac{l_g(l_g + 1)\hbar^2}{2mR_E^2} \quad (\text{A1})$$

with  $\delta R = R_B - R_E$ , where  $R_E$  is the position of the barrier for  $l = l_g$  (see Eq. (12)). Because the first derivative of the total potential is zero at the barrier position, we

also have

$$0 = \frac{Z_1 Z_2 e^2}{R_B^2} e^{\delta R/a} - \frac{Z_1 Z_2 e^2}{R_E^2} - \frac{l_g(l_g + 1)\hbar^2}{m R_E^3}. \quad (\text{A2})$$

By combining these two equations, it can be shown that  $\delta R$  satisfies

$$e^{\delta R/a} = 1 + \frac{E - B + \frac{1}{2}V_{CB}[1 + \delta R/R_B - (1 - \delta R/R_B)^{-1}]}{B - \frac{1}{2}V_{CB}(1 + \delta R/R_B)}, \quad (\text{A3})$$

where  $V_{CB}$  is again the Coulomb potential at  $R_B$ , the position of the  $l = 0$  barrier.

Inserting  $\delta R = 0$  on the right-hand side of this equation, one obtains

$$e^{\delta R/a} = 1 + \frac{E - B}{B - \frac{1}{2}V_{CB}} \quad (\text{A4})$$

and from this first-order approximation to  $\delta R$  we obtain (c.f. Ref.[18])

$$R_E = R_B - a \ln \left( 1 + \frac{E - B}{B - \frac{1}{2}V_{CB}} \right). \quad (\text{A5})$$

Eq. (A3) can be easily iterated and rapidly converges to the exact result for  $R_E$ .

The top panel of Fig. 14 shows a comparison between the exact value of  $R_E$  (solid line) with those obtained in first order (Eq. (A5)) and second order (dotted and dashed lines respectively) for the  $^{12}\text{C}+^{12}\text{C}$  system. The middle and the bottom panels show  $V_E$  and  $\hbar\omega_E$  used in the energy-dependent Wong formula (14), evaluated at the corresponding exact and approximate  $R_E$  values. One can see that the first-order formula given by Eq. (A5) works well only at energies in the vicinity of the  $s$ -wave Coulomb barrier, where  $\delta R$  is small. The second-order result already leads to excellent results over the entire energy range shown, and higher orders converge rapidly to the exact result.

## Appendix B: Derivation of oscillatory term

In this appendix, we give a detailed derivation of Eqs. (16) and (19). First we note that the Hill-Wheeler formula for the transmission,

$$T(E, \lambda) = \frac{1}{1 + \exp \left[ \frac{2\pi}{\hbar\omega} \left( B - E + \frac{\lambda^2 \hbar^2}{2mR^2} \right) \right]}, \quad (\text{B1})$$

has poles at the complex angular momenta  $\lambda$  which satisfy

$$\exp \left[ \frac{2\pi}{\hbar\omega} \left( B - E + \frac{\lambda^2 \hbar^2}{2mR^2} \right) \right] = -1 = e^{i(\pi + 2n\pi)}, \quad (\text{B2})$$

with  $n = 0, \pm 1, \pm 2, \dots$ . To find the poles nearest to the real axis with  $n = 0$  and  $-1$ , we put  $\lambda_{\text{pole}} = \lambda_g + i\lambda_I$ ,

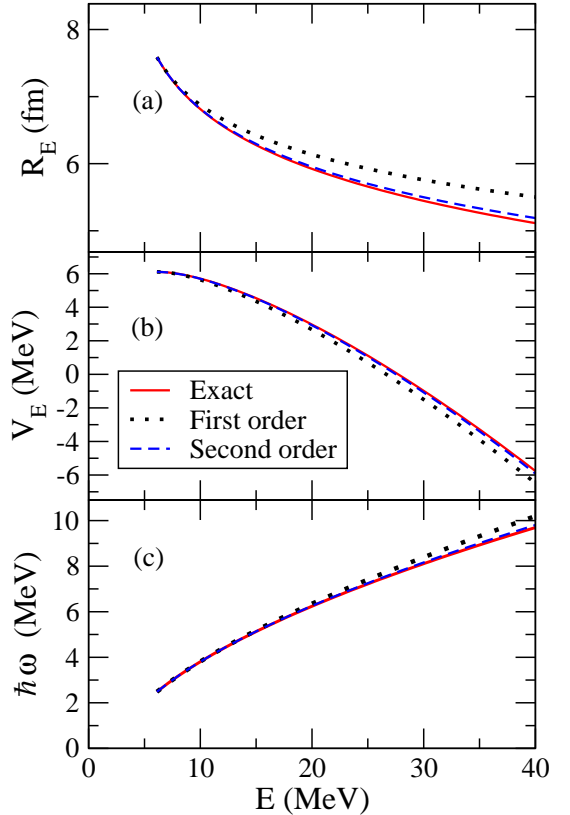


FIG. 14: (Color online) (a) exact and approximate barrier positions  $R_E$  for the  $^{12}\text{C}+^{12}\text{C}$  system as a function of the incident energy  $E$ . An exponential nuclear potential with the diffuseness parameter  $a=0.8$  fm has been used. The solid line shows the exact value obtained with Eq. (A3), while the dotted and the dashed lines are obtained from Eq. (A5) in first- and second-order respectively. (b) as (a) but for the value of the  $s$ -wave potential at  $R_E$ . (c) same for the curvature of the barrier for the grazing angular momentum  $l_g$ .

and neglecting the second-order term in  $\lambda_I$ , we find from Eq. (B2) that  $\lambda_g$  and  $\lambda_I$  satisfy

$$B - E + \frac{\lambda_g^2 \hbar^2}{2mR^2} = 0, \quad (\text{B3})$$

and

$$\lambda_I \sim \pm \frac{\hbar\omega}{2\lambda_g} \cdot \frac{mR^2}{\hbar^2}. \quad (\text{B4})$$

In the vicinity of the poles, the denominator of the right hand side of Eq. (B1) is given by

$$\begin{aligned} & 1 + \exp \left[ \frac{2\pi}{\hbar\omega} \left( B - E + \frac{\lambda^2 \hbar^2}{2mR^2} \right) \right] \\ & \sim -\frac{2\pi}{\hbar\omega} \cdot \frac{\lambda_{\text{pole}} \hbar^2}{mR^2} (\lambda - \lambda_{\text{pole}}), \end{aligned} \quad (\text{B5})$$

where we have used Eq. (B2) to derive this equation.

We are now ready to evaluate the  $m = \pm 1$  terms in the Poisson summation formula (15) by contour integration.

From the contour enclosing the upper, right quadrant of the complex plane, we may write the  $m = 1$  term as

$$\sigma_1 = -\frac{2\pi}{k^2} \int_0^\infty \lambda T(E, \lambda) e^{2\pi i \lambda} d\lambda, \quad (\text{B6})$$

$$= -\frac{2\pi}{k^2} \left[ -2\pi i \lambda_{\text{pole}}^{(+)} \frac{\hbar\omega}{2\pi} \frac{mR^2}{\lambda_{\text{pole}}^{(+)} \hbar^2} e^{2\pi i \lambda_{\text{pole}}^{(+)}} \right. \\ \left. - \int_\infty^0 (i\tilde{\lambda}) T(E, i\tilde{\lambda}) e^{-2\pi i \tilde{\lambda}} (id\tilde{\lambda}) \right], \quad (\text{B7})$$

where  $\lambda_{\text{pole}}^{(+)}$  takes the positive sign in Eq. (B4). Here, we neglect the second term of this equation; as  $T$  is real and  $< 1$  on the imaginary axis, the integral is real and  $< (2\pi)^{-2}$  and merely gives a very small correction to the smooth part of the cross section. So one finds

$$\sigma_1 = i \frac{2\pi \hbar\omega}{k^2} \frac{mR^2}{\hbar^2} e^{2\pi i \lambda_g} e^{-\pi \frac{\hbar\omega}{\lambda_g} \frac{mR^2}{\hbar^2}}. \quad (\text{B8})$$

Similarly for the  $m = -1$  term we have

$$\sigma_{-1} = i \frac{2\pi \hbar\omega}{k^2} \frac{mR^2}{\hbar^2} e^{-2\pi i \lambda_g} e^{-\pi \frac{\hbar\omega}{\lambda_g} \frac{mR^2}{\hbar^2}}. \quad (\text{B9})$$

Combining Eqs. (B8) and (B9) and using  $\sin(2\pi\lambda_g) = \sin(2\pi l_g + \pi) = -\sin(2\pi l_g)$ , one finally obtains Eq. (16).

With identical particles the fusion cross sections must be symmetrized and are given by

$$\sigma = \frac{\pi}{k^2} \sum_l (2l+1) T_l(E) (1 \pm (-1)^l), \quad (\text{B10})$$

$$= \frac{2\pi}{k^2} \sum_{m=-\infty}^{m=\infty} (-1)^m \int_0^\infty \lambda d\lambda T(E, \lambda) e^{2\pi m i \lambda} (1 \mp ie^{i\pi\lambda}), \quad (\text{B11})$$

where the positive sign in Eq. (B10) relates to the spatially symmetric case and the negative sign to the spatially anti-symmetric case. The symmetrization is seen to lead to two terms,  $m = 0$  and  $m = -1$ , where the exponent is reduced by a factor 2. These terms now clearly dominate, and the fusion cross sections are approximately given by

$$\sigma = \frac{2\pi}{k^2} \int_0^\infty \lambda d\lambda T(E, \lambda) (1 \mp ie^{i\pi\lambda}) \\ \pm \frac{2\pi}{k^2} \int_0^\infty \lambda d\lambda T(E, \lambda) e^{-i\pi\lambda}. \quad (\text{B12})$$

One can evaluate these integrals as above, and using  $\cos(\pi\lambda_g) = -\sin(\pi l_g)$ , we obtain

$$\sigma = \sigma_{\text{Wong}} \pm \sigma_{\text{osc}}, \quad (\text{B13})$$

where the considerably enhanced oscillatory term is now given by Eq. (19).

In the above proof, we have used energy-independent values for  $B$ ,  $R$  and  $\hbar\omega$  for simplicity of notation. However, the results are easily generalised to the energy-dependent case, when the above total cross section is given by Eqs. (14) and (19) using  $V_E$ ,  $R_E$  and  $\hbar\omega_E$ . (More generally these quantities depend on the angular momentum rather than the energy, see discussion in Sec. III).

---

[1] P. Sperr, T.H. Braid, Y. Eisen, D.G. Kovar, F.W. Prosser Jr., J.P. Schiffer, S.L. Tabor and S.E. Vigdor, Phys. Rev. Lett. **37**, 321 (1976).

[2] P. Sperr, S. Vigdor, Y. Eisen, W. Henning, D.G. Kovar, T.R. Ophel and B. Zeidman, Phys. Rev. Lett. **36**, 405 (1976); J.J. Kolata, R.M. Freeman, F. Haas, B. Heusch and A. Gallmann, Phys. Lett. **65B**, 333 (1976).

[3] B. Fernandez, C. Gaarde, J.S. Larsen, S. Pontoppidan and F. Videbaek, Nucl. Phys. **A306**, 259 (1978); J.J. Kolata, R.M. Freeman, F. Haas, B. Heusch and A. Gallmann, Phys. Rev. C**19**, 2237 (1979).

[4] H. Esbensen, Phys. Rev. C**85**, 064611 (2012).

[5] C.Y. Wong Phys. Rev. C**86**, 064603 (2012).

[6] C.Y. Wong, Phys. Rev. Lett. **31**, 766 (1973).

[7] D.L. Hill and J.A. Wheeler, Phys. Rev. **89**, 1102 (1953).

[8] C. Simenel, R. Keser, A.S. Umar and V.E. Oberacker, Phys. Rev. C**88**, 024617 (2013).

[9] N. Poffé, N. Rowley and R. Lindsay, Nucl. Phys. **A410**, 498 (1983).

[10] K. Hagino, N. Rowley and A.T. Kruppa, Comp. Phys. Comm. **123**, 143 (1999).

[11] R. Bass, *Nuclear Reactions with Heavy Ions* (Springer-Verlag, New York, 1980).

[12] Ö. Akyüz and A. Winther, in *Nuclear Structure and Heavy-Ion Collisions*, Proceedings of the International School of Physics “Enrico Fermi,” Course LXXVII, Varenna, 1979, edited by R.A. Broglia *et al.* (North-Holland, Oxford, 1981).

[13] N. Rowley, H. Doubre and C. Marty, Phys. Lett. **69B**, 147 (1977).

[14] Y. Kondo, B.A. Robson and R. Smith, Phys. Lett. **B227**, 310 (1989).

[15] Y. Kondo, F. Michel and G. Reidemeister, Phys. Lett. **B242**, 340 (1990).

[16] N. Rowley, G.R. Satchler and P.H. Stelson, Phys. Lett. **B254**, 25 (1991).

[17] M. Dasgupta, D.J. Hinde, N. Rowley and A.M. Stefanini, Annu. Rev. Nucl. Part. Sci. **48**, 401 (1998).

[18] N. Rowley, A. Kabir and R. Lindsay, J. Phys. G **15**, L269 (1989).

- [19] K. Hagino, N. Rowley and M. Dasgupta, Phys. Rev. C**67**, 054603 (2003).
- [20] K. Hagino and N. Takigawa, Prog. Theo. Phys. **128**, 1061 (2012).
- [21] N. Rowley, N. Grar and M. Trotta, Phys. Rev. C**76**, 044612 (2007).
- [22] D.M. Brink, *Semi-Classical Methods for Nucleus-Nucleus Scattering*, (University Press, Cambridge, 1985).
- [23] A. Kabir, M.W. Kermode and N. Rowley, Nucl. Phys. **A481**, 94 (1988).
- [24] W. von Oertzen, Nucl. Phys. **A148**, 529 (1970).
- [25] W. von Oertzen and H.G. Bohlen, Phys. Rep. **19**, 1 (1975).
- [26] M. Lozano and A. Vitturi, Phys. Rev. C**35**, 367 (1987).
- [27] A. Vitturi and C.H. Dasso, Nucl. Phys. **A458**, 157 (1986).
- [28] J.A. Christley, M.A. Nagarajan and A. Vitturi, Nucl. Phys. **A591**, 341 (1995).
- [29] M. F. Vineyard *et al.*, Phys. Rev. C 41, 1005 (1990).
- [30] S. Gary and C. Volant, Phys. Rev. C 25, 1877 (1982).
- [31] Y. Nagashima *et al.*, Phys. Rev. C 33, 176 (1986).
- [32] E.F. Aguilera *et al.*, Phys. Rev. C 33, 1961 (1986).
- [33] A.M. Stefanini, G. Montagnoli, L. Corradi, S. Courtin, E. Fioretto, J. Grebosz, F. Haas, H.M. Jia, M. Mazzocco, C. Michelagnoli, T. Mijatovic, D. Montanari, C. Parascondolo, F. Scarlassara, E. Strano, S. Szilner, D. Torresi and C.A. Ur, EPJ Web of Conf. **66**, 03082 (2014).
- [34] I. Wiedenhöver *et al.*, Phys. Rev. Lett. **87**, 14250 (2001).
- [35] S. M. Harris, Phys. Rev. **138**, B509 (1965); Phys. Rev. Lett. **13**, 663 (1964).
- [36] N. Takigawa, K. Hagino, M. Abe and A.B. Balantekin, Phys. Rev. C**49**, 2630 (1994).
- [37] K. Hagino, N. Takigawa, M. Dasgupta, D.J. Hinde, and J.R. Leigh, Phys. Rev. Lett. **79**, 2014 (1997).
- [38] P. Sperr *et al.*, Phys. Rev. Lett. **37**, 321 (1976). D.G. Kovar *et al.*, Phys. Rev. C**20**, 1305 (1979).
- [39] M. Yasue *et al.*, Nucl. Phys. **A394**, 29 (1983).
- [40] D. Baye, Nucl. Phys. **A460**, 581 (1986).
- [41] Y. Kondo, B.A. Robson and R. Smith, Nucl. Phys. **A410**, 289 (1983).
- [42] T. Spillane *et al.*, Phys. Rev. Lett. **98**, 122501 (2007).
- [43] M. Notani *et al.*, Phys. Rev. C**85**, 014607 (2012).
- [44] C.L. Jiang *et al.*, Phys. Rev. Lett. **110**, 072701 (2013).
- [45] For  $a \ll R_C$  this gives the very simple relation  $R_B \approx R_C - a$ , though we shall not use this approximation in this paper.
- [46] The ground-state rotational band of  $^{24}\text{Mg}$  is well fitted up to the highest identified spin of Ref. [34] ( $I^\pi=10^+$  at 19.2 MeV) by the Harris parametrization [35] with  $\mathcal{J}_0=2.22 \text{ } \hbar^2 \cdot \text{MeV}^{-1}$  and  $\mathcal{J}_1=0.115 \text{ } \hbar^4 \cdot \text{MeV}^{-3}$ . This gives the energies  $E_{12+}=25.80 \text{ MeV}$ ,  $E_{14+}=33.05 \text{ MeV}$ ,  $E_{16+}=40.85 \text{ MeV}$ ..., and so forth.